ACS APPLIED MATERIALS & INTERFACES

Research Article

www.acsami.org

Self-Assembly of Tetrakis (3-Trifluoromethylphenoxy) Phthalocyaninato Cobalt(II) on Multiwalled Carbon Nanotubes and Their Amperometric Sensing Application for Nitrite

Pan Li,† Yu Ding,† Ao Wang, Lin Zhou, Shaohua Wei,* Yiming Zhou, Yawen Tang, Yu Chen,* Chenxin Cai, and Tianhong Lu

Jiangsu Key Laboratory of Power Batteries, Laboratory of Electrochemistry, School of Chemistry and Materials Science, Nanjing Normal University, 1# Wenyuan Road, Nanjing 210023, PR China

ABSTRACT: In this work, the soluble cobalt phthalocyanine functionalized multiwalled carbon nanotubes (MWCNTs) are synthesized by $\pi-\pi$ stacking interaction between tetrakis (3-trifluoromethylphenoxy) phthalocyaninato cobalt(II) (CoPcF) complex and MWCNTs. The physical properties of CoPcF-MWCNTs hybrids are evaluated using spectroscopy (UV−vis, XPS, and Raman) and electron microscopy (TEM and SEM). Subsequently, an amperometric nitrite electrochemical sensor is designed by immobilizing CoPcF-MWCNTs hybrids on the glassy carbon electrode. The immobilized CoPcF complex shows the fast electron transfer rate and excellent electrocatalytic activity for the oxidation of nitrite. Under optimum experimental conditions, the proposed nitrite electrochemical sensor shows the fast response (less than 2 s), wide linear range (9.6×10^{-8} to 3.4×10^{-4} M) and low detection limit (6.2×10^{-8} M) because of the good mass transport, fast electron transfer rate, and excellent electrocatalytic activity.

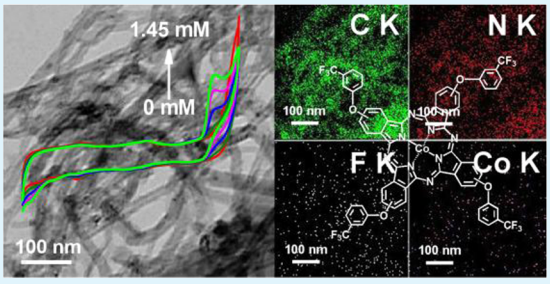

KEYWORDS: *cobalt phthalocyanine, carbon nanotubes, nitrite, electrocatalysis, sensor*

1. INTRODUCTION

Nitrite is ubiquitous within environment, food and physiological systems because it is commonly used as an food addiitive, dyeing agent, and corrosion inhibitor. Moreover, it also plays a key physiological role in signaling, blood flow regulation, hypoxic nitric oxide homeostasis, and cancer.[1−15] Thus, the determination of nitrite is very important both in environmental and biological aspects. Numerous methods such as chromatography,[1] chemiluminescence,[2] spectrophotometry,[3] molecular absorption spectrometry,[4] fluorescence,[5] capillary electrophoresis,[6] and electrochemistry[7−15] have been reported for the quantification of trace amount of nitrite. Among them, electrochemical methods have been widely used because of their considerable advantages such as simplicity, rapid response, high sensitivity, and ease of miniaturization.[7−15] However, the direct determination of nitrite at bare electrode generally suffers from a large overpotential. Therefore, various chemically modified electrodes by immobilizing the electrocatalysts have been explored to lower the operating potential for nitrite sensing.[7−15]

Carbon nanotubes (CNTs), a relatively new carbon material, have unique one-dimensional geometric structure, high electric conductivity, large accessible surface area, excellent chemical stability, and good corrosion resistance, which makes these excellent candidates for basic scientific study of material science.[16−19] Metallo-phthalocyanine (MPc) complexes, a well-known class of N4-macrocyclic metal compounds with the planar 18 π-conjugated skeleton, have intriguing physical and chemical properties as well as widely technological applications such as sensing and electrocatalysis.[20,21] One of the current research interests in phthalocyanine chemistries is the integration of CNTs with MPc (simply called MPc-CNTs hybrids).[20] Recent reports demonstrate that MPc-CNTs hybrids exhibit enhanced electrochemical activity in comparison to the use of CNTs or MPc alone for many electrochemical reactions.[22−25]

At present, the practical applications of phthalocyanine compounds (Pcs) are extremely limited due to the poor solubility in organic solvent and water, originating from their strong stacking propensity. To improve solubility, Pcs are generally modified by introducing various solubility-enhancing substituents at the peripheral and axial positions of Pcs ring. In our previous work, we have found that the introduction of the trifluoromethlphenoxy group with strong electron-withdrawing property into the peripheral position of phthalocyanines could impart high solubility of MPc in organic solvents.[26] On the other hand, it is known that the applications of pristine MWCNTs are also extremely limited because of the insolubility, originating from their inert graphitic nature, strong hydrophobicity, and strong intertube van der Waals inter-

Received: January 13, 2013
Accepted: March 2, 2013
Published: March 2, 2013

actions.[27,28] In this work, we synthesized soluble tetrakis (3-trifluoromethylphenoxy) phthalocyaninato cobalt(II) (CoPcF) functionalized multiwalled carbon nanotubes (MWCNTs) in dimethylformamide (DMF), and subsequently fabricated an amperometric nitrite electrochemical sensor. The morphology and structure of CoPcF-MWCNTs hybrids were characterized by scanning electron microscopy (SEM), transmission electron microscopy (TEM), X-ray photoelectron spectroscopy (XPS), ultraviolet and visible spectroscopy (UV−vis), and Raman spectroscopy. The direct electrochemistry and electrocatalysis of the modified electrode were investigated using various electrochemical techniques including cyclic voltammetry, multipotential step, and chronoamperometry.

2. EXPERIMENTAL SECTION

2.1. Reagents and Chemicals. Multiwalled carbon nanotubes (MWCNTs, >95% purity) were purchased from Chengdu Organic Chemicals Co. Ltd. Tetrakis (3-trifluoromethylphenoxy) phthalocyaninato cobalt(II) (CoPcF, shown in Scheme 1) was was synthesized

Scheme 1. Structure of the CoPcF Complex

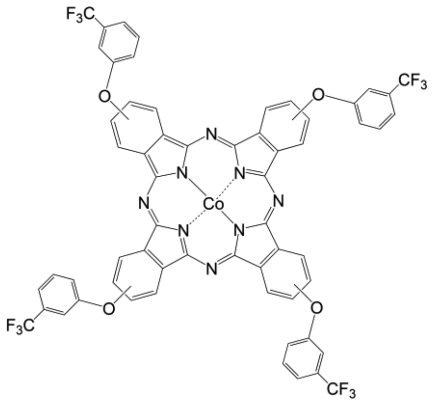

according to the previous work reported by us.[26] IR (cm^{-1}): 1654, 1610, 1591, 1490, 1449, 1408 (C−F), 1326 (C−F), 1281, 1234 (Ar−O−Ar), 1168, 1123, 1062, 975, 909, 825, 793, 696, 654. Element analysis: ($C_{60}H_{28}CoF_{12}N_8O_4$, FW 1211) Cal: C 59.47, H2.33, N 9.25; Found: C 59.44, H 2.23, N 9.15. Stock solution of $NaNO_2$ was freshly prepared before use. All other reagents were of analytical grade and used without further purification. Phosphate buffer solutions (PBS, 0.1 M, pH 7.0) were prepared by mixing standard stock solutions of K_2HPO_4 and KH_2PO_4.

2.2. Preparation of the CoPcF-MWCNT/GC Electrode. The soluble CoPcF-MWCNT hybrids in DMF were synthesized through the $\pi-\pi$ stacking interaction between MWCNTs and CoPcF. In brief, 3 mg of pristine MWCNTs were added into 1 mL of 5 mM CoPcF DMF solution, and then sonicated in ice water for 2 h. After filtration and washing, CoPcF-MWCNT hybrids were obtained.

0.6 mg of as-prepared CoPcF-MWCNT hybrids were dispersed in 0.2 mL of DMF to give a black suspension of 3 mg mL^{-1}. The suspension was essentially stable. No precipitation or flocculation is observed even after 6 months. Then 4 μL of mixture was dropped onto the precleaned glassy carbon (GC, 3 mm in diameter) electrode and allowed to dry at ambient temperature. The fabricated electrode was denoted as the CoPcF-MWCNTs/GC electrode and stored at room temperature when not in use. For comparison, the CoPcF/GC and MWCNTs/GC electrodes were also fabricated by the similar procedures.

2.3. Instruments. XPS was performed on a Thermo VG Scientific ESCALAB 250 spectrometer with a Mg Kα radiator. UV−vis spectra were recorded on a UV3600 spectrophotometer. TEM images were taken using a JEOL 2000 transmission electron microscopy operated at 200 kV. SEM was performed on a Hitachi S4800 scanning electron microscopy. Raman spectra were examined with a Labram HR 800 UV Raman spectrometer. All electrochemical experiments were performed on a CHI 660B electrochemical analyzer at 25 ± 1 ∘C. A three-electrode system, including a working CoPcF-MWCNTs/GC electrode, a saturated calomel reference electrode (SCE), and a platinum wire counter electrode, was employed. All potentials in this study were reported with respect to SCE. The electrolyte was purged with high purity nitrogen for at least 10 min prior to measurements to remove the dissolved oxygen unless otherwise stated.

3. RESULTS AND DISCUSSION

3.1. Characterization of CoPcF-MWCNT Hybrids. It is clear that MPc can adsorb firmly on graphite at monolayer levels through strong $\pi-\pi$ interaction.[21] The evidence for the modification of MWCNTs was determined by UV−vis. The absorption spectrum of CoPcF in DMF is typical for nonaggregated MPc (Figure 1a).[29,30] It shows a broad B

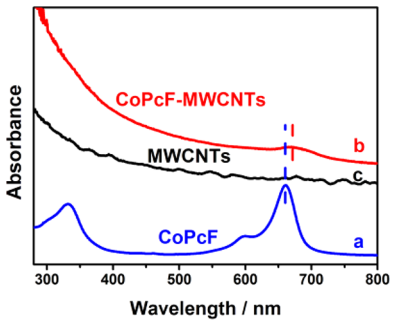

Figure 1. UV−vis spectra of (a) CoPcF, (b) CoPcF-MWCNTs hybrids, and (c) pristine MWCNTs.

band at 332 nm, an intense and sharp Q-band at 661 nm, together with a vibronic band at 600 nm. Likely, the steric hindrance of peripheral 3-trifluoromethlphenoxy substituents makes it impossible to form dimers of CoPcF. Meanwhile, the characteristic Q-band of CoPcF is also observed for CoPcF-MWCNTs hybrids (Figure 1b), further indicating the successful self-assembly of CoPcF on MWCNTs. However, the B-band and the vibronic band of CoPcF can not be observed for CoPcF-MWCNTs hybrids. As observed, the pristine MWCNTs have obvious absorption in 800−280 nm (Figure 1c), which interferes with absorption of CoPcF complex and consequently results in the disappearance of the B-band and vibronic band of CoPcF in CoPcF-MWCNTs hybrids. With reference to CoPcF spectrum, red shifts for Q-band appears in the spectrum of CoPcF-MWCNTs hybrids (from 661 to 669 nm), originating from the charge transfer from phthalocyanine ring to MWCNTs.[24,31,32]

XPS was used to monitor the characteristic elements of the CoPcF and to confirm the self-assembly of CoPcF on MWCNTs. The appearance of Co2p and F1s peaks indicates the formation of CoPcF-MWCNTs hybrids (Figure 2), which is not observed in the spectrum of pristine MWCNTs (data not shown). The content of element Co at CoPcF-MWCNTs hybrids is measured to be about 0.4 at.% by XPS analysis. Moreover, it is observed that the binding energies of Co and F atoms in CoPcF-MWCNTs hybrids are higher than those in CoPcF (Figure 2). This discrepancy indicates that the introduction of MWCNTs reduces the electron density around the Co and F nuclei in CoPcF. The occurrence of the charge transfer from CoPcF to MWCNTs should be taken into consideration properly.[24,32]

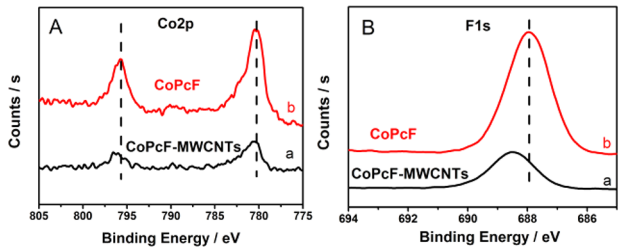

Figure 2. XPS spectra of (a) CoPcF-MWCNTs hybrids and (b) CoPcF in (A) the Co 2p and (B) F 1s regions, respectively.

The morphology of CoPcF-MWCNTs hybrids was investigated by TEM. Compared with pristine MWCNTs (Figure 3A), CoPcF complex located outside of CoPcF-MWCNTs

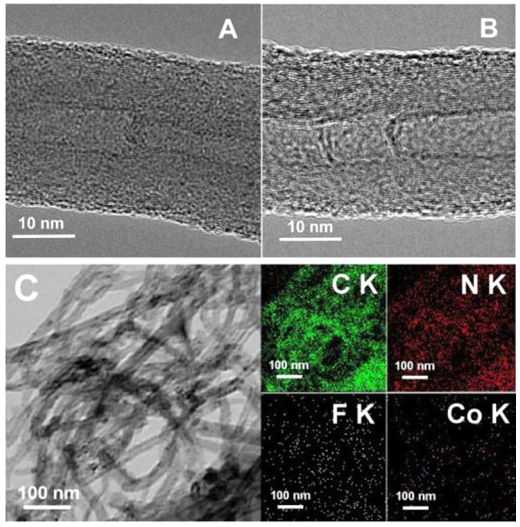

Figure 3. TEM images of (A) pristine MWCNTs and (B) CoPcF-MWCNTs hybrids. (C) Representative large-area TEM image of CoPcF-MWCNTs hybrids and corresponding energy dispersive spectrum mapping.

hybrids is not visible (Figure 3B), which may be indicative of monolayer adsorption of CoPcF on MWCNTs. However, the large-area energy dispersive spectrum mapping shows that N, Co, and F elements are distributed evenly in whole MWCNTs (Figure 3C), indicating the uniform distribution of CoPcF on MWCNTs.

Noncovalent functionalization of CNTs can effectively preserve the atomic and electronic structures of CNTs compared to the chemical modification of CNTs.[33] Figure 4

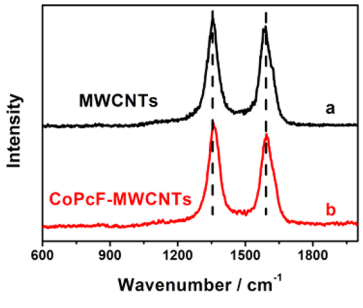

Figure 4. Raman spectra of (a) pristine MWCNTs and (b) CoPcF-MWCNTs hybrids.

shows Raman spectra of pristine MWCNTs and CoPcF-MWCNTs hybrids. Both samples exhibit two characteristic peaks at ca. 1356 and 1592 cm^{-1}, corresponding to the D band and G band. It is well-known that the intensity ratio of the D band to G band (i.e., I_D/I_G) can directly indicate the structural changes of CNTs.[34] The I_D/I_G value of CoPcF-MWCNTs hybrids is very close to that of pristine MWCNTs (1.13 vs 1.09). The fact indicates CoPcF-MWCNTs hybrids retain the electronic and structural integrity of pristine MWCNTs, which is in favor of electron transfer in electrochemical reaction.

The soluble CoPcF-MWCNTs hybrids in DMF is insoluble in water (Figure 5A), which facilitates the successful application

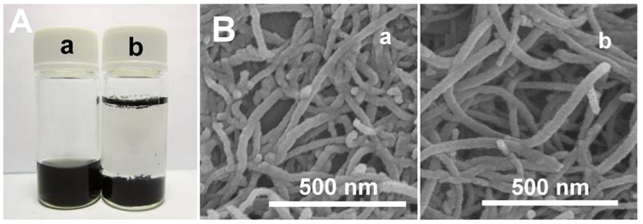

Figure 5. (A) Photographs of CoPcF-MWCNTs hybrids suspension in DMF (a) before and (b) after addition of water. (B) SEM images of (a) MWCNTs/GC and (b) CoPcF-MWCNTs/GC electrodes.

of the CoPcF-MWCNTs/GC electrode in water system (i.e., no leakage or exfoliation). The surface morphologies of MWCNTs/GC and CoPcF-MWCNTs/GC electrodes were investigated by SEM. Similar to MWCNTs/GC electrode (Figure 5B-a), the CoPcF-MWCNTs/GC electrode also shows the three-dimensionally network-like structure (Figure 5B-b). Obviously, the interconnected MWCNTs can provide continuous conducting pathways for the transportation of electron. Meanwhile, the three-dimensional configuration can essentially increase electrode area and facilitate mass transport of analytes, and consequently increase the sensitivity of electrochemical response.[35−39] These characteristics are beneficial for the fabrication of electrochemical sensors.

3.2. Electrochemistry of the CoPcF-MWCNTs/GC Electrode. Electrochemical properties of modified electrodes were investigated by cyclic voltammetry. Two couple of typical redox peaks appear at the CoPcF-MWCNTs/GC electrode with formal potentials of +0.021 and −0.47 V (Figure 6A-a), whereas these two couple of peaks are invisible at the MWCNTs/GC electrode (Figure 6A-b), suggesting that CoPcF is responsible for those peaks. According to previous

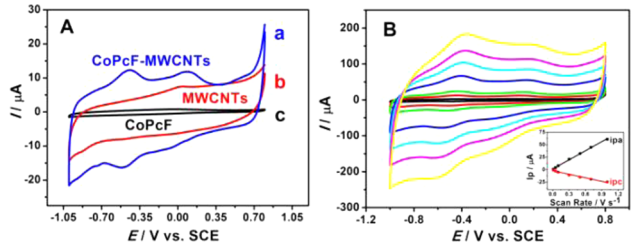

Figure 6. (A) Cyclic voltammograms of (a) CoPcF-MWCNTs/GC, (b) MWCNTs/GC, and (c) CoPcF/GC electrodes in N_2-saturated 0.1 M PBS at a scan rate of 50 mV s^{-1}. (B) Cyclic voltammograms of CoPcF-MWCNTs/GC in N_2-saturated 0.1 M PBS at different scan rates. Inset: plots of the corresponding cathodic and anodic peak currents at −0.47 V vs scan rate.

dx.doi.org/10.1021/am400152k | ACS Appl. Mater. Interfaces 2013, 5, 2255−2260

study, the redox peaks at +0.021 and −0.47 V are assigned to the redox couples of Co(III)/Co(II)[40,41] and Co(II)/Co(I),[42−45] respectively. It is clear that the electrocatalytic activity of MPc highly depends on the central metal atom and the structure of phthalocyanine molecule. Suitable modifications in *Pc* molecules can remarkably influence the redox potential of MPc, and consequently improve their electrocatalytic properties. Compared with previous reports, the formal potential of Co center in CoPcF positively shifts 130 mV,[42,46] originating from strong electron-withdrawing property of trifluoromethlphenoxy group.[47,48] In addition, no redox peaks are observed at CoPcF/GC electrode (Figure 6A-c). This fact indicates the direct electron transfer of CoPcF is promoted by MWCNTs, which may be ascribed to charge transfer between CoPcF and MWCNTs. With the increase of scan rate, the formal potential of the CoPcF-MWCNTs/GC electrode is almost unchanged, while the anodic and cathodic peak currents increase linearly (Figure 6B), showing a surface-controlled electrode reaction. For a surface process, according to Laviron's equation, the charge-transfer rate constant of the CoPcF at CoPcF-MWCNTs/GC electrode is estimated to be 3.31 s^{-1} at a scan rate of 1 V s^{-1}.

3.3. Electrocatalysis and Determination of Nitrite. The electrocatalytic activity of the CoPcF-MWCNTs/GC electrode was first investigated by cyclic voltammetry. With the addition of nitrite, a new anodic peak at 0.76 V appears, and peak current increase with nitrite concentration (Figure 7A),

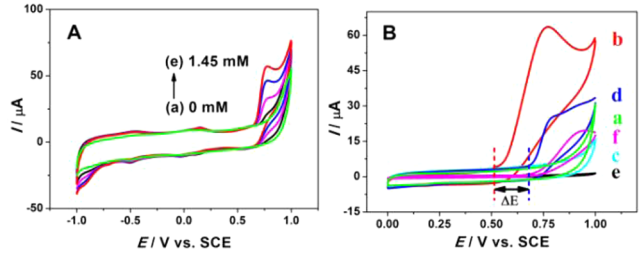

Figure 7. (A) Cyclic voltammograms of the CoPcF-MWCNTs/GC electrode in N_2-saturated 0.1 M PBS containing (a) 0, (b) 0.36, (c) 0.72, (d) 1.09, and (e) 1.45 mM $NaNO_2$ at a scan rate of 50 mV s^{-1}. (B) Cyclic voltammograms of (a, b) the CoPcF-MWCNTs/GC electrode, (c, d) MWCNTs/GC electrode, and (e, f) naked GC electrode in the (a, c, e) absence and (b, d, f) presence of 1.45 mM $NaNO_2$ in N_2-saturated 0.1 M PBS at a scan rate of 50 mV s^{-1}.

showing a typical electrocatalytic oxidation process of nitrite. The controlled experiments demonstrate that the GC and MWCNTs/GC electrodes have the lower electrocatalytic activities toward the oxidation of nitrite compared to the CoPcF-MWCNTs/GC electrode (Figure 7B). For example, the oxidation current of nitrite at the CoPcF-MWCNTs/GC electrode is 2.83 times bigger than that at the MWCNTs/GC electrode at 0.76 V. Moreover, the onset potential of nitrite oxidation at the CoPcF-MWCNTs/GC electrode negatively shifts ca. 170 mV compared to that at the MWCNTs/GC electrode. The lower onset oxidation potential and higher oxidation current show that the CoPcF-MWCNTs hybrids have higher electrocatalytic performance than MWCNTs, suggesting CoPcF complex has excellent electrocatalytic activity toward the oxidation of nitrite. According to previous reports, the electrocatalytic oxidation[49,50] or reduction[51] of nitrite on iron(III) porphyrin complexes is a typical EC (electrochemical and chemical) catalytic process. Because of the similarity of molecular structure between polyporphyrin and phthalocyanin, we presume the following two-step mechanism is responsible for the electrocatalytic oxidation of nitrite on CoPcF: The interaction between nitrite and CoPcF is shown in eq 1, which involves the interaction of an adduct where nitrite is located in an axial position, as a fifth ligand of the Co center of CoPcF. The formation of NO_2 (eq 2) is followed by the disproportionation of the nitrogen dioxide to give nitrite and nitrate (see eqs 3 and 4) and therefore, nitrate is the sole product.[49] In addition, a new cathodic peak at −0.9 V is also observed clearly after addition of nitrite, which is ascribed to the reduction of nitrite. In fact, the electrochemical determination of nitrite can be achieved by reduction or oxidation of nitrite. Because reduction of nitrite usually suffers from known interferences from nitrate and molecular oxygen, oxidation determination of nitrite is preferred.[52]

$$Co^{III}(PcF) + NO_2^- \rightleftharpoons [Co^{III}(PcF)(NO_2^-)] \quad (1)$$

$$[Co^{III}(PcF)(NO_2^-)] \rightleftharpoons Co^{III}(PcF) + NO_2 + e^- \quad (2)$$

$$2NO_2 + H_2O \rightleftharpoons 2H^+ + NO_3^- + NO_2^- \quad (3)$$

$$NO_2^- + H_2O \rightleftharpoons 2H^+ + NO_3^- + 2e^- \quad (4)$$

To investigate the effect of applied potential on nitrite oxidation current, the multipotential step test was performed.[18,36,53] As shown in Figure 8, the detection potentials

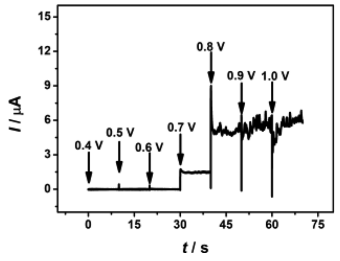

Figure 8. Background subtracted multipotential step curve of the CoPcF-MWCNTs/GC electrode in N_2-saturated 0.1 M PBS containing 0.15 mM $NaNO_2$. Step increase: 0.1 V; step time: 10 s.

determine the sensitivity of detection. Within the potential range of 0.4−0.8 V, the steady-state current of nitrite oxidation increases considerably with applied potential. Moving the applied potential to positive values further, the nitrite oxidation current does not increase accordingly. Thus, an applied potential of 0.8 V is selected as the optimized value for chronoamperometry.

Figure 9A shows the amperometric detection of nitrite at 0.8 V. Upon addition of $NaNO_2$, oxidation current increases rapidly and sensitively. And the response time, considering the time to reach 95% of the steady state signal, is approximately 2 s. The corresponding calibration plot shows the current response and the concentration of $NaNO_2$ has a linear relationship in the concentration range from 9.6×10^{-8} to 3.4×10^{-4} M with a correlation coefficient of 0.996 (Figure 9B), which is much wider than earlier reports.[7,8,11,14,26,29,52,54,55] The linear regression equation is expressed as i_{pa} (μA) = 0.5231 + 0.0299 c (μM). The detection limit of 6.2×10^{-8} M is estimated at a signal-to-noise ratio of three. Such an excellent quantitative analysis of nitrite was rarely reported in the previous works. Thus, it is concluded that the CoPcF-MWCNTs/GC electrode can be used to construct electro-

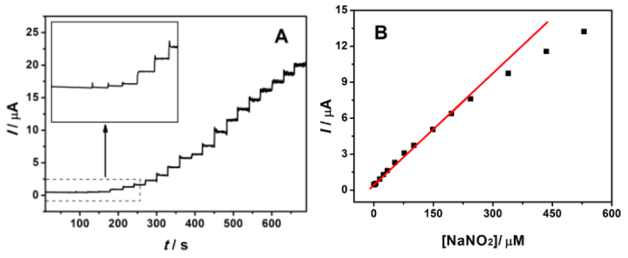

Figure 9. (A) Dynamic amperometric response of the CoPcF-MWCNTs/GC electrode at a working potential of 0.8 V with successive injections of $NaNO_2$ in air-saturated 0.1 M PBS under continuous stirring. (B) Corresponding calibration plot of the current response and the concentration of $NaNO_2$.

chemical sensor toward the determination of nitrite. Reproducibility was checked by recording the amperometric response of 50 μM $NaNO_2$ for eight measurements and the relative standard deviations were found to be less than 3.0%. Furthermore, the interference study indicated that 5 mM Cl^-, Br^-, NO_3^-, ClO_4^-, SO_4^{2-}, CO_3^{2-}, Li^+, and K^+ ions did not interfere with the detection of 50 μM of $NaNO_2$, which could be explained exclusively by the above-mentioned electrocatalytic oxidation mechanism of nitrite because these ions did not react with Co center of the CoPcF under the same conditions. After 30 days of storage in air, the electrode could retain ca. 96% of its initial response for 50 μM $NaNO_2$. This fact indicated the modified electrode had excellent stability, which was attributed to the excellent self-stabilities of the CoPcF and MWCNTs.

4. CONCLUSIONS

The CoPcF could self-assemble on MWCNTs by $\pi-\pi$ stacking interaction. MWCNTs promoted the direct electron transfer of CoPcF due to strong $\pi-\pi$ stacking interaction. The strong electron-withdrawing property of trifluoromethlphenoxy group resulted in positive shift of formal potential of CoPcF. The high insolubility of CoPcF-MWCNTs hybrids in water was in favor of the successful application of the CoPcF-MWCNTs/GC electrode in water system (i.e., no leakage or exfoliation). The modified electrode offered excellent electrocatalytic activity for the oxidation of nitrite. Therefore, the CoPcF-MWCNTs/GC electrode was employed to detect nitrite, and the wide linear range (9.6×10^{-8} to 3.4×10^{-4} M) and the low detection limit (6.2×10^{-8} M) were obtained. Besides, the modified electrode showed an inherent stability, fast response time, and good anti-interference ability. These suggested that the CoPcF-MWCNTs/GC electrode was favorable and reliable for the detection of nitrite.

AUTHOR INFORMATION

Corresponding Author

*E-mail: weishaohua@njnu.edu.cn (S.W.); ndchenyu@yahoo.cn (Y.C.).

Author Contributions

†P.L. and Y.D. contributed equally to this work.

Notes

The authors declare no competing financial interest.

ACKNOWLEDGMENTS

The authors are grateful for the financial support of National "973" program of China (2012CB215500), NSFC (20973093, 21073094, 21005039, 21273116, and 21201102), and a project funded by the Priority Academic Program Development of Jiangsu Higher Education Institutions.

REFERENCES

(1) Ito, K.; Nomura, R.; Fujii, T.; Tanaka, M.; Tsumura, T.; Shibata, H.; Hirokawa, T. *Anal. Bioanal. Chem.* **2012**, *404*, 2513−2517.
(2) Yaqoob, M.; Biot, B. F.; Nabi, A.; Worsfold, P. J. *Luminescence* **2012**, *27*, 419−425.
(3) Pourreza, N.; Fathi, M. R.; Hatami, A. *Microchem. J.* **2012**, *104*, 22−25.
(4) Brandao, G. C.; Lima, D. C.; Ferreira, S. L. C. *Talanta* **2012**, *98*, 231−235.
(5) Wang, L. L.; Li, B.; Zhang, L. M.; Zhang, L. G.; Zhao, H. F. *Sens. Actuators, B* **2012**, *171*, 946−953.
(6) Erdogan, B. Y.; Onar, A. N. *J. Food Drug Anal.* **2012**, *20*, 532−538.
(7) Silveira, G.; de Morais, A.; Villis, P. C. M.; Maroneze, C. M.; Gushikem, Y.; Lucho, A. M. S.; Pissetti, F. L. *J. Colloid Interface Sci.* **2012**, *369*, 302−308.
(8) Li, X. R.; Liu, J.; Kong, F. Y.; Liu, X. C.; Xu, J. J.; Chen, H. Y. *Electrochem. Commun.* **2012**, *20*, 109−112.
(9) Ge, X. B.; Wang, L. Q.; Liu, Z. N.; Ding, Y. *Electroanal.* **2011**, *23*, 381−386.
(10) Lin, C. Y.; Balamurugan, A.; Lai, Y. H.; Ho, K. C. *Talanta* **2010**, *82*, 1905−1911.
(11) Azad, U. P.; Ganesan, V. *Chem. Commun.* **2010**, *46*, 6156−6158.
(12) Ding, Y.; Wang, Y.; Li, B. K.; Lei, Y. *Biosens. Bioelectron.* **2010**, *25*, 2009−2015.
(13) Li, X. R.; Kong, F. Y.; Liu, J.; Liang, T. M.; Xu, J. J.; Chen, H. Y. *Adv. Funct. Mater.* **2012**, *22*, 1981−1988.
(14) Liang, F. F.; Jia, M. Z.; Hu, J. B. *Electrochim. Acta* **2012**, *75*, 414−419.
(15) Wang, J. Y.; Diao, P.; Zhang, Q. *Analyst* **2012**, *137*, 145−152.
(16) Zheng, M.; Li, P.; Fu, G.; Chen, Y.; Zhou, Y.; Tang, Y.; Lu, T. *Appl. Catal., B* **2013**, *129*, 394−402.
(17) Zhang, F.; Zhang, L.; Xing, J.; Tang, Y.; Chen, Y.; Zhou, Y.; Lu, T.; Xia, X. *ChemPlusChem* **2012**, *77*, 914−922.
(18) Li, P.; Liu, H.; Ding, Y.; Wang, Y.; Chen, Y.; Zhou, Y.; Tang, Y.; Wei, H.; Cai, C.; Lu, T. *J. Mater. Chem.* **2012**, *22*, 15370−15378.
(19) Chen, Y.; Zhang, G.; Ma, J.; Zhou, Y.; Tang, Y.; Lu, T. *Int. J. Hydrogen Energy* **2010**, *35*, 10109−10117.
(20) Agboola, B. O.; Ozoemena, K. I.; Nyokong, T.; Fukuda, T.; Kobayashi, N. *Carbon* **2010**, *48*, 763−773.
(21) Silva, J. F.; Griveau, S.; Richard, C.; Zagal, J. H.; Bedioui, F. *Electrochem. Commun.* **2007**, *9*, 1629−1634.
(22) Wolfbeis, O. S.; Durkop, A.; Wu, M.; Lin, Z. *Angew. Chem., Int. Ed.* **2002**, *41*, 4495−4498.
(23) Zuo, X.; Li, N.; Zhang, H.. *J. Mater. Sci.* **2012**, *47*, 2731−2735.
(24) Zhao, H.; Zhang, Y.; Zhao, B.; Chang, Y.; Li, Z. *Environ. Sci. Technol.* **2012**, *46*, 5198−5204.
(25) Wu, P.; Cai, Z.; Chen, J.; Zhang, H.; Cai, C. *Biosensor. Bioelectron.* **2011**, *26*, 4012−4017.
(26) Dong, S.; Li, N.; Huang, T.; Tang, H.; Zheng, J. *Actuators B, Chem.* **2012**, *173*, 704−709.
(27) Doe, C. W.; Choi, S. M.; Kline, S. R.; Jang, H. S.; Kim, T. H. *Adv. Funct. Mater.* **2008**, *18*, 2685−2691.
(28) Yang, Q.; Pan, X. J. *Ind. Eng. Chem. Res.* **2010**, *49*, 2747−2751.
(29) Sun, W.; Li, X.; Wang, Y.; Zhao, C.; Jiao, K. *Bioelectrochemistry* **2009**, *75*, 170−175.
(30) Zhao, B.; Liu, Z.; Liu, G.; Li, Z.; Wang, J.; Dong, X. *Electrochem. Commun.* **2009**, *11*, 1707−1710.
(31) Mamuru, S. A.; Ozoemena, K. I.; Fukuda, T.; Kobayashi, N.; Nyokong, T. *Electrochim. Acta* **2010**, *55*, 6367−6375.
(32) Yang, Y.; Xu, L.; Li, F.; Du, X.; Sun, Z. *J. Mater. Chem.* **2010**, *20*, 10835−10840.
(33) Fagnoni, M.; Profumo, A.; Merli, D.; Dondi, D.; Mustarelli, P.; Quartarone, E. *Adv. Mater.* **2009**, *21*, 1761−1765.

(34) Datsyuk, V.; Kalyva, M.; Papagelis, K.; Parthenios, J.; Tasis, D.; Siokou, A.; Kallitsis, I.; Galiotis, C. *Carbon* **2008**, *46*, 833−840.
(35) Zhao, J.; Zhu, M.; Zheng, M.; Tang, Y.; Chen, Y.; Lu, T. *Electrochim. Acta* **2011**, *56*, 4930−4936.
(36) Chen, Y.; Yang, X. J.; Guo, L. R.; Li, J.; Xia, X. H.; Zheng, L. M. *Anal. Chim. Acta* **2009**, *644*, 83−89.
(37) Zheng, M.; Zhou, Y.; Chen, Y.; Tang, Y.; Lu, T. *Electrochim. Acta* **2010**, *55*, 4789−4798.
(38) Wieckowska, A.; Wisniewska, M.; Chrzanowski, M.; Kowalski, J.; Korybut-Daszkiewicz, B.; Bilewicz, R. *Pure Appl. Chem.* **2007**, *79*, 1077−1085.
(39) Dong, B.; He, B. L.; Huang, J.; Gao, G. Y.; Yang, Z.; Li, H. L. *J. Power Sources* **2008**, *175*, 266−271.
(40) Yin, H. S.; Zhou, Y. L.; Ai, S. Y. *J. Electroanal. Chem.* **2009**, *626*, 80−88.
(41) Obirai, J. C.; Nyokong, T. *J. Electroanal. Chem.* **2007**, *600*, 251−256.
(42) Pereira-Rodrigues, N.; Cofre, R.; Zagal, J. H.; Bedioui, F. *Bioelectrochemistry* **2007**, *70*, 147−154.
(43) Griveau, S.; Albin, V. U.; PauportU, T.; Zagal, J. U. H.; Bedioui, F. *J. Mater. Chem.* **2002**, *12*, 225−232.
(44) Griveau, S.; Pavez, J.; Zagal, J. H.; Bedioui, F. *J. Electroanal. Chem.* **2001**, *497*, 75−83.
(45) Griveau, S.; Gulppi, M.; Pavez, J.; Zagal, J. H.; Bedioui, F. *Electroanal.* **2003**, *15*, 779−785.
(46) YU-HONG, T.; Janda, P.; HERMAN, L.; Zhang, J.; WILLIAM, J. P.; Lever, A. *J. Porphyrins Phthalocyanines* **1997**, *1*, 3−16.
(47) Koc, I.; Ozer, M.; Ozkaya, A. R.; Bekaroglu, O. *Dalton Trans.* **2009**, *32*, 6368−6376.
(48) Guo, J.; Li, H.; He, H.; Chu, D.; Chen, R. *J. Phys. Chem. C* **2011**, *115*, 8494−8502.
(49) Armijo, F.; Goya, M. C.; Reina, M.; Canales, M. J.; Arevalo, M. C.; Aguirre, M. *J. Mol. Catal. A: Chem.* **2007**, *268*, 148−154.
(50) Chen, J.; Ikeda, O.; Hatasa, T.; Kitajima, A.; Miyake, M.; Yamatodani, A. *Electrochem. Commun.* **1999**, *1*, 274−277.
(51) Chi, Y.; Chen, J.; Aoki, K. *Inorg. Chem.* **2004**, *43*, 8437−8446.
(52) Eguilaz, M.; Agui, L.; Yanez-Sedeno, P.; Pingarron, J. *J. Electroanal. Chem.* **2010**, *644*, 30−35.
(53) Liang, Y.; Zhou, Y.; Ma, J.; Zhao, J.; Chen, Y.; Tang, Y.; Lu, T. *Appl. Catal., B* **2011**, *103*, 388−396.
(54) Zhang, L. Y.; Yi, M. *Bioproc. Biosyst. Eng.* **2009**, *32*, 485−492.
(55) Zhang, W.; Yuan, R.; Chai, Y. Q.; Zhang, Y.; Chen, S. H. *Sens. Actuators, B* **2012**, *166*, 601−607.